Soil matrix study using a hybrid a-Se/CMOS pixel detector for CT scanning

Akyl Swaby[a], Adam S. Wang[b], Michael G. Farrier[c], Weixin Cheng[d], and Shiva Abbaszadeh[a]

[a]Electrical and Computer Engineering, University of California, Santa Cruz, 1156 High St., Santa Cruz, CA, USA, 95064;
[b]Department of Radiology, Stanford University, 300 Pasteur Dr., Stanford, CA, USA, 94305;
[c]Farrier Microengineering LLC, 616 Petoskey St., Unit 004, Petoskey, MI, USA, 49770;
[d]Environmental Studies, University of California, Santa Cruz, 1156 High St., Santa Cruz, CA, USA, 95064

*This work has not been previously submitted for publication or presentation elsewhere.

ABSTRACT

Computed tomography (CT) is a non-invasive means of localizing a region of interest within an object, which enables the investigation of soil distributions and localized flow processes within soil pore systems. CT scanning allows for cross-sectional successions that provide visibility within the environment of plant samples. Knowledge of the characteristics of the soil pore system is essential for evaluating various processes that take place between root-soil interactions. In this study, we investigate the potential application of a high-resolution amorphous selenium (a-Se) direct conversion detector on complementary metal-oxide-semiconductor (CMOS) readouts for micro-CT scanning of a soil matrix to image the status of aggregation and networks of pore spaces within intact soil. The combination of the intrinsic high spatial resolution of a-Se and small pixel CMOS readouts provide detailed visualization in the soil aggregates of the plant samples. The X-ray energy and plant soil thickness were varied during the investigation for imaging the root-soil. A 10 µm spatial resolution and noise limited performance of 8 photons/pixel at 20 keV were achieved. High attenuation of X-rays in thick soil poses challenges however fine details are observable in thinner samples and care should be taken when choosing soil thickness and container material.

Keywords: Amorphous selenium, computed tomography, radiation imaging, soil properties.

1. INTRODUCTION

X-ray computed tomography (CT) is implemented to characterize and visualize the environment of plant samples for the investigation of the physical and hydrological properties related to root-soil interactions. The use of CT scanning for characterization of the impact of pore spaces within a soil matrix has been previously studied [1-3]. These studies have demonstrated the advantages of using CT scanning for the characterization of soil aggregate properties such as volume, surface area, and sphericity enabled by the non-destructive quantification of soil structures as three dimensional (3D) images. Imaging the soil structures, which are described as the aggregation or distribution and networks of pore spaces, provides visibility into the root-soil interactions that affect the pore structure within the rhizosphere. The rhizosphere is the site of interaction between the plant root and the soil where water and nutrients are absorbed by the roots and where photosynthates are distributed [4]. CT scanning presents many advantages including the ability to rotate the 3D images and to view their cross-sectional slices, making it efficient to locate the regions of interest in the rhizosphere of the plant. Visibility within the sample and the relatively high spatial resolution of CT images combined with positron emission tomography (PET) allow for the investigation of the temporal changes occurring in the plant, soil, and root tips due to the transport of a radiation tracer, such as Carbon-11 (^{11}C) attached to CO_2 [4].

Previous investigations using CT for studying the root-soil interactions have highlighted challenges such as [5-10]:

(i) scale integration from the micron scale to the ecosystem scale of the rhizosphere; and

(ii) a lack of dynamic observations/measurements of soil structural changes in response to disturbances at various temporal scales.

7th International Conference on Image Formation in X-Ray Computed Tomography,
edited by Joseph Webster Stayman, Proc. of SPIE Vol. 12304, 123041E
 · 0277-786X · doi: 10.1117/12.2646496

To enable a low cost, high spatial resolution X-ray detector towards real-time CT scanning of plants combined with dynamic PET imaging, we are investigating replacing the indirect conversion scintillator detector with a direct conversion photoconductive layer made of amorphous selenium (a-Se). Easily processed as a uniform thick layer over large areas, a-Se has an atomic number (Z = 34) sufficient for high absorption of X-ray imaging (20-100 keV), a k-edge energy of 12.66 keV, low dark current, high charge collection efficiency, and high inherent spatial resolution [11, 12]. In this study, we investigate the impact of using a hybrid a-Se/CMOS coupled to an active pixel array for X-ray imaging.

2. METHODS

A preliminary experiment was conducted at Stanford University using the Siemens Artis Zeego [13] with a tube voltage range of 40 – 125 kV, a 210 mA current, and 11.5 ms pulse width. The X-ray tube within the system is a Megalix Cat 125/15/40/80 three-focus high-performance X-ray tube assembly. The X-ray detector has an indirect conversion layer composed of amorphous silicon (a-Si) with a cesium iodide (CsI) scintillation material. The detector consists of an area of 30 × 40 cm^2 with a pixel size of 154 µm [14]. The CT projection images were collected at 30 images per second, for a total of 496 projections.

A sample root-soil system (Fig. 1) was imaged within an acrylic container (10 × 10 × 12 cm^3; L × W × H). At the time of the imaging, the Calypso beans (*Phaseolus vulgaris*, cultivar 'Calypso') were grown for three weeks after germination with soil moisture ranging from 50% to 80% field capacity.

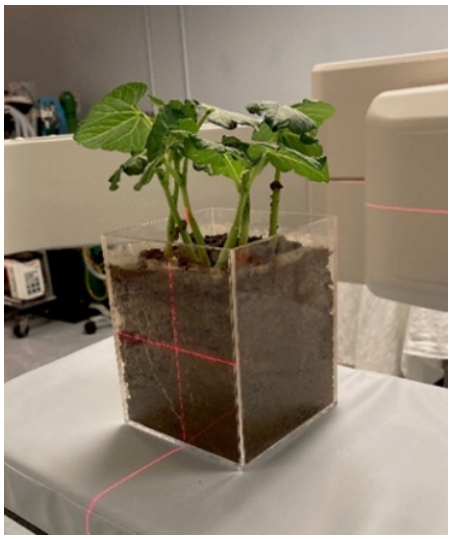

Figure 1. A sample of a root-soil system imaged to study soil aggregates.

In comparison to the images from the Artis Zeego CT system, the 1-Megapixel (1Mp) X-ray detector can acquire images of the plant sample with finer detailed information of the roots and soil structure. A performance summary of the detector is listed in Table 1 [15]:

Table 1. Summary of the a-Se/CMOS direct conversion X-ray detector performance specifications.

Detector features	**Values**
Pixel size	7.8 µm
Array size	1000 × 1000 pixels
Field of view	7.8 mm × 7.8 mm
Frame rate max	5 fps
Full well capacity	877 ke$^-$
RMS noise	180 e$^-$ @ 5fps
Conversion gain	762 e$^-$/ph @ 63 keV, 120 e$^-$/ph @ 20 keV, 5 V/µm
System conversion	90.6 e$^-$/DN (theoretical)
MTF (Modulation transfer function)	50% @ 0.5 Nyq. (32 lp/mm) @ 63 keV @ 5 V/µm
Detector field (HV)	4 to > 10 V/µm
Image Lag	1% to 3% @ 1s

The test bench for investigating the hybrid a-Se detector included a microfocus X-ray source (Microbox, Micro X-ray Inc. (MXR), Santa Cruz) and the 1Mp X-ray detector. The MXR microfocus X-ray source has a varying focal spot size ranging from 5 µm to 10 µm as the source output power changes from 7.5 to 15 W. Developed by KA Imaging, the 1Mp X-ray detector is an a-Se/CMOS hybrid structure with 1000 × 1000 pixels (Fig. 2) [16]. The key technology consists of a monolithic hybrid X-ray detector built by layering an a-Se film directly deposited on each 7.8 µm pixel of the CMOS active pixel readout array [15]. This a-Se/CMOS direct X-ray detector technology has demonstrated micron scale resolution as well as an order of magnitude increase in detection efficiency from typical indirect X-ray detectors at energies ranging from 15 keV to > 63 keV [16].

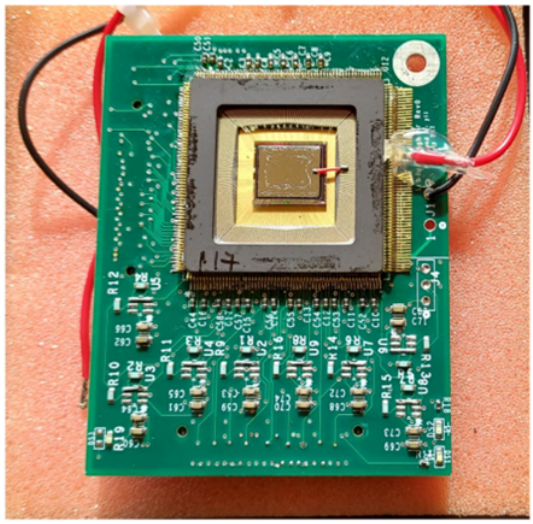

Figure 2. Photo of the 1Mp a-Se/CMOS Hybrid Detector with a 7.8 µm pixel pitch. The 1Mp detector package and analog daughter board are soldered to the test board.

The CMOS readout integrated circuit (ROIC) design of the 1Mp detector has the potential to become scalable in array size, using reticle stitching IC fabrication technology, to achieve an array greater than 8000 × 8000 = 64 megapixels, with FOV greater than 63 × 63 mm^2. Due to the limited size of the chip, in order to scan a larger sample, repeated scans of the sample will be necessary as well as combining the acquisition images as the FOV

would be limited by the size of the pixel array.

3. RESULTS

Figure 3 shows the CT images taken at Stanford University, using the Siemens Artis Zeego, at an average energy of 97 kV vs 109 kV, 512 × 512 voxel array, and 0.49 vs 0.25 mm voxel sizes. The Artis Zeego C-arm was positioned with respect to the orientation of the potted plant, using the laser traces to align the sample. Due to its design, the C-arm has a non-continuous axis of rotation that was accounted for in the reconstruction. Parameters that were set for acquisition and reconstruction included tube voltage, dose, automatic exposure control (AEC) field, VOI (volume of interest) size, reconstruction kernel, and slice matrix, while parameters that were automatically selected included tube current and pulse width.

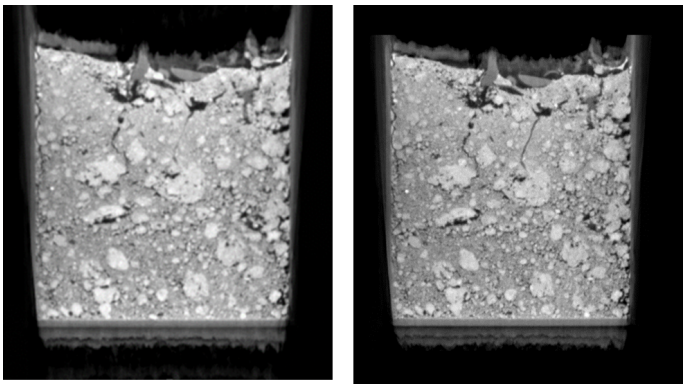

(a) (b)

Figure 3. Image reconstruction of the Calypso sample with (a) average tube voltage of 97 keV and 0.49 voxel size [mm] and (b) average 109 keV and 0.25 voxel size [mm].

Using the 1Mp detector and MXR micro focus X-ray source, images were acquired at an energy of 20 kV using a 900 × 900 pixel array. The microfocus X-ray source emits at a spot size that is matched to the detector pixel pitch to minimize penumbral blurring. Figure 4 shows an image acquired from grass roots with a thickness of 0.5 cm to 0.75 cm at an energy of 20 kV with a 1:1 magnification. To improve contrast of the roots in the soil, soil-root samples were contained between Kapton films to visualize the biomass. At low kV energy, significant structural detail in the grass roots can be visualized and detected at a 15 µm to 23 µm resolution.

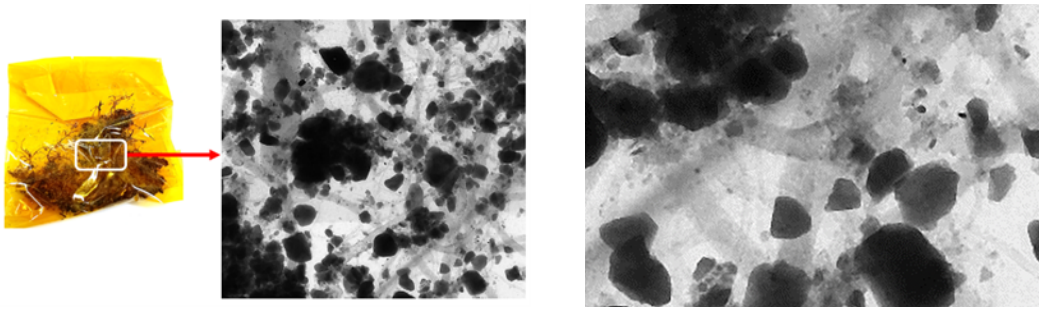

(a) (b)

Figure 4. (a) Image of grass roots in soil with a sample thickness of 0.5 cm to 0.75 cm. The image was acquired using a 900 × 900 pixel array from the 1Mp detector, equivalent to an active area of 7 × 7 mm^2. (b) A detail of the grass root sample using 2 to 3 pixels, from the detector, provides a resolution of 15 µm to 23 µm at 1:1 magnification.

Further imaging of plant root samples demonstrates significant structural detail visible at a 10 µm to 15 µm resolution (Fig. 5). However, attenuation in soil substantially obscures the low-density biomass structure. As it can be seen from Fig. 6, the low-density target made of food-grade polypropylene (PP) plastic emulating the low density of the biomass materials was obscured by soil material. A 5 mm thickness of soil absorbs more than 80% of X-ray photons at 20 kV. Figure 7 shows the X-ray penetration vs. soil thickness at 60 kV. It can be seen that 10 mm of soil absorbs 60% of X-ray photons at 60 kV.

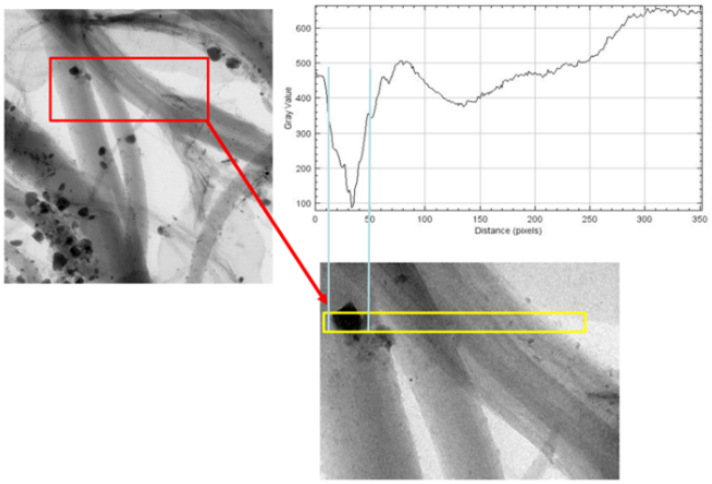

Figure 5. Image of a live plant root sample used to study the attenuation of X-ray signal through soil material. The attenuation in soil substantially obscures the low-density biomass structure. The graph shows the gray scale of the acquired image versus the distance equivalent to the number of pixels of the detector.

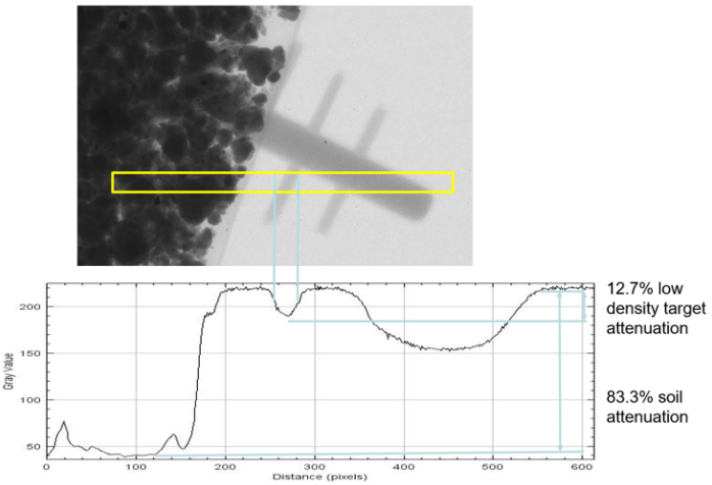

Figure 6. Image of soil material obscuring a low-density target (food-grade polypropylene (PP) plastic) with a tube voltage of 20 kV. The plastic target was used to simulate a low-density biomass target which demonstrated that 5 mm of soil absorbs more than 80% of X-ray photons at 20 kV. The graph shows the gray scale of the acquired image versus the distance equivalent to the number of pixels of the detector.

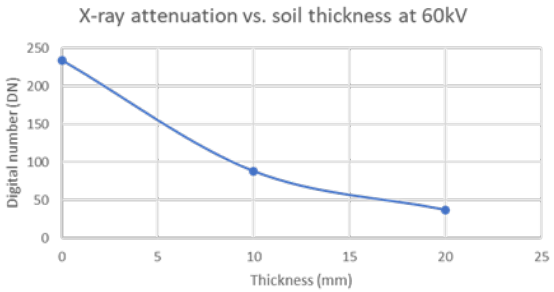

Figure 7. X-ray attenuation study vs. soil thickness. 10 mm of soil absorbs 60% at 60 kV.

4. DISCUSSION

Details in the rhizosphere provided by a higher resolution image may allow for modelling of representative interacting volumes of root hairs and soil particles [17, 18]. The percentage of porous area can be calculated from the images shown in Fig. 3. A high resolution image can be utilized to determine the correlation between where roots continue to grow and the porosity of the soil. Compared to the pixel size of 154 µm in the Artis Zeego detector, the 7.8 µm pixel size of the a-Se detector provides improved resolution which is needed for studying the finer structure of microaggregates (with diameters ranging from 10 µm to 250 µm) and the micropores inside microaggregates. More importantly, many crucial functions provided by plant roots, microorganisms, and soil aggregates normally operate at this finer resolution.

From initial imaging of plant samples within an acrylic container, it was observed that the acrylic container in combination with soil is absorbing X-ray at low energies, causing limited image quality of the rhizosphere. As previously investigated, considering X-ray CT with energy information, the X-ray energy distribution can be calculated using a mathematical model, such as a response function, to obtain reference measurements of the optimal thickness for the X-ray path length in an acrylic container [19].

5. CONCLUSION

Based on previous investigations related to the study of root-soil characteristics using X-ray CT scanning [5-10], we have investigated the use of a direct conversion CMOS ROIC, the 1Mp detector, to improve the image quality and resolution of the pixel detector currently implemented in the Artis Zeego. CMOS direct charge sensors may be capable of improving the limitations caused by the ratio between sample size and resolution (voxel size), as well as the smaller resolution for larger sample sizes [20]. The combination of high spatial resolution and high quality image reconstruction may allow for improved detail in the image quality of the 3D acquisition of the rhizosphere. From this preliminary work, the X-ray source emitted at a spot size that is matched to the detector pixel pitch to minimize penumbral blurring. A 10 µm spatial resolution and noise limited performance of 8 photons/pixel at 20 keV were achieved. We believe that microCT of live plants, in situ, would require:

i) A high fluence, high keV X-ray source that would generate images of voids in the soil where biomass in growing.

ii) A form of radio dense metallic dopant to be taken up in the root system.

The combined application of PET and CT scanning may provide simultaneous spatial and temporal data on root morphology and architecture.

ACKNOWLEDGMENTS

We acknowledge support from the US Department of Energy (DOE), Office of Biological and Environmental Research (BER) under Award No. DE-SC0021975. Detector development was also funded through DOE, Office of Science, phase I SBIR program, grant No. DE-SC0019626.

REFERENCES

[1] Grevers, M. C. J., Jong, E. D., St. Arnaud, R. J. (1989). The characterization of soil macroporosity with CT scanning. Canadian Journal of Soil Science, 69(3), 629-637.

[2] Warner, G. S., Nieber, J. L., Moore, I. D., Geise, R. A. (1989). Characterizing macropores in soil by computed tomography. Soil Science Society of America Journal, 53(3), 653-660.

[3] Garbout, A., Munkholm, L. J., Hansen, S. B. (2013). Temporal dynamics for soil aggregates determined using X-ray CT scanning. Geoderma, 204, 15-22.

[4] Garbout, A., Munkholm, L. J., Hansen, S. B., Petersen, B. M., Munk, O. L., Pajor, R. (2012). The use of PET/CT scanning technique for 3D visualization and quantification of real-time soil/plant interactions. Plant and soil, 352(1), 113-127.

[5] Hou, L. H., Gao, W., Weng, Z. H., Doolette, C. L., Maksimenko, A., Hausermann, D., ... Kopittke, P. M. (2022). Use of X-ray tomography for examining root architecture in soils. Geoderma, 405, 115405.

[6] Naveed, M., Moldrup, P., Schaap, M. G., Tuller, M., Kulkarni, R., Vogel, H. J., Wollesen de Jonge, L. (2016). Prediction of biopore-and matrix-dominated flow from X-ray CT-derived macropore network characteristics. Hydrology and Earth System Sciences, 20(10), 4017-4030.

[7] Peyton, R. L., Haeffner, B. A., Anderson, S. H., Gantzer, C. J. (1992). Applying X-ray CT to measure macropore diameters in undisturbed soil cores. Geoderma, 53(3-4), 329-340.

[8] Singh, J., Singh, N., Kumar, S. (2020). X-ray computed tomography–measured soil pore parameters as influenced by crop rotations and cover crops. Soil Science Society of America Journal, 84(4), 1267-1279.

[9] Sun, X., Li, X., Zheng, B., He, J., Mao, T. (2020). Study on the progressive fracturing in soil and rock mixture under uniaxial compression conditions by CT scanning. Engineering Geology, 279, 105884.

[10] Helliwell, J. R., Sturrock, C. J., Mairhofer, S., Craigon, J., Ashton, R. W., Miller, A. J., ... Mooney, S. J. (2017). The emergent rhizosphere: imaging the development of the porous architecture at the root-soil interface. Scientific reports, 7(1), 1-10.

[11] Allec, N., Abbaszadeh, S., Fleck, A., Tousignant, O., Karim, K. S. (2012). K-edge imaging using dual-layer and single-layer large area flat panel imagers. IEEE Transactions on Nuclear Science, 59(5), 1856-1861.

[12] Hellier, K., Benard, E., Scott, C. C., Karim, K. S., Abbaszadeh, S. (2021). Recent Progress in the Development of a-Se/CMOS Sensors for X-ray Detection. Quantum Beam Science, 5(4), 29.

[13] Siemens Healthineers — Corporate Home. Accessed December 10, 2021. https://www.siemens-healthineers.com/

[14] System Description. zeego@Stanford Lab. Accessed December 10, 2021. https://med.stanford.edu/zeegolab/instrument/system.html

[15] Scott, C. C., Farrier, M., Li, Y., Laxer, S., Ravi, P., Kenesei, P., ... Karim, K. S. (2021). High-energy micrometre-scale pixel direct conversion X-ray detector. Journal of Synchrotron Radiation, 28(4).

[16] Farrier MG, Scott C, Karim KS, Con C, Li Y. High Energy Micron Scale Pixel Hybrid Detector. Farrier Microengineering LLC, Boyne City, MI; 2019. doi:10.2172/1576188

[17] Keyes, S. D., Daly, K. R., Gostling, N. J., Jones, D. L., Talboys, P., Pinzer, B. R., ... Roose, T. (2013). High resolution synchrotron imaging of wheat root hairs growing in soil and image based modelling of phosphate uptake. New Phytologist, 198(4), 1023-1029.

[18] Daly, K. R., Keyes, S. D., Masum, S., Roose, T. (2016). Image-based modelling of nutrient movement in and around the rhizosphere. Journal of experimental botany, 67(4), 1059-1070.

[19] Minami, Y., Imamura, R., Kanno, I., Ohtaka, M., Hashimoto, M., Ara, K., Onabe, H. (2011). Using x-ray energy information in CT measurement of a phantom with an Al region. Journal of nuclear science and technology, 48(1), 108-112.

[20] Pajor, R., Falconer, R., Hapca, S., Otten, W. (2010). Modelling and quantifying the effect of heterogeneity in soil physical conditions on fungal growth. Biogeosciences, 7(11), 3731-3740.